JOURNAL OF AGRICULTURAL AND FOOD CHEMISTRY

Optimization of Lipase-Catalyzed Synthesis of Acetylated Tyrosol by Response Surface Methodology

IMEN AISSA,[†,‡] MOHAMED BOUAZIZ,[‡] HANEN GHAMGUI,[†] AMEL KAMOUN,[§] NABIL MILED,[†] SAMI SAYADI,[‡] AND YOUSSEF GARGOURI*[,†]

Laboratoire de Biochimie et de Génie Enzymatique des Lipases, ENIS route de Soukra, 3038 Sfax-Tunisia, Laboratoire des Bioprocédés, Centre de Biotechnologie de Sfax, BP « K », 3038, Sfax, Tunisie, and Laboratoire de Chimie Industrielle II, ENIS route de Soukra, 3038 Sfax-Tunisia

The ability of a noncommercial immobilized lipase from *Staphylococcus xylosus* (SXL_i) to catalyze the transesterification of tyrosol and ethyl acetate was investigated. Response surface methodology was used to evaluate the effects of the temperature (40–60 °C), the enzyme amount (50–500 UI), and the ethyl acetate/hexane volume ratio (0.2–1) on the tyrosol acetylation conversion yield. Two independent replicates were carried out under the optimal conditions predicted by the model (reaction temperature 54 °C, enzyme amount 500 UI, and volume ratio ethyl acetate/ hexane 0.2). The maximum conversion yield reached 95.36 ± 3.6%, which agreed with the expected value (96.8 ± 3.7%). The ester obtained was characterized by spectroscopic methods. Chemical acetylation of tyrosol was performed, and the products were separated using HPLC. Among the eluted products from HPLC, mono- and diacetylated derivatives were identified by positive mass spectrometry. Tyrosol and its monoacetylated derivative exert similar antiradicalar activity on 2,2-diphenyl-1-picrylhydrazyle.

KEYWORDS: Acetylation; antioxidant; immobilized *Staphylococcus xylosus* lipase; response surface methodology

INTRODUCTION

Polyphenolic compounds produced by plants are of considerable research interest, both as functional food ingredients and as nutraceuticals, because of their antioxidant properties (*1*) and other beneficial biological activities (*2*). Extra-virgin olive oil is the principal fat component of the Mediterranean diet, and its chemical constituents have been intensively studied (*3, 4*). The main olive oil phenols are oleuropein, tyrosol, and hydroxytyrosol. It has been reported that the tyrosol has scavenging effects on $ONOO^-$ (*5*) and O^{2-} (*6*). In addition to its antioxidative effects, it has been shown that tyrosol inhibits lipopolysaccharide (LPS)-induced cytokine release from human monocytes (*7*) and the activity of the leukocyte 5-lipoxygenase release in human mononuclear cells (*8*). Furthermore, previous studies have suggested that tyrosol has an anti-inflammatory effect in vitro (*9*), fully protected Caco-2 cells against the cytotoxic/apoptotic effects of oxLDL (*10*), and a neuroprotective effect in the stroke rat model (*11*). Recently, it has been determined that tyrosol penetrates and accumulates in macrophages and improves the intracellular antioxidant defense systems (*12*). A recent increase in serious research on the commercial application of radical scavengers as beneficial antiaging and photoprotection ingredients in cosmetic products (*13, 14*), and the demand for nontoxic antioxidants that are active in hydrophilic and lipophilic systems, led to the additional focus on new natural antioxidants that can be used in oil-based formulas and emulsions. The acetylation of biophenols increases their hydrophobicity and, therefore, lipid solubility and may modify their bioavailability (*15*), antioxidant effect in food emulsions (*16*), stability, and color stability (*17*). This acetylation can be explored by reaction with acid chlorides or acid anhydrides, but these routes do not meet the requirements necessary for food applications. We can overcome the disadvantages by the use of enzymes in nonaqueous media. Guyot et al. (*18*) have reported for the first time the enzymatic esterification of phenolic acid and alcohols with lipase from *Candida antartica* B. Then, Buisman et al. (*19*) studied the esterification of cinnamic acid and some benzoic acid derivatives with fatty alcohols varying between 4 and 12 carbon atoms (C_4–C_{12}). Recently, the hydroxytyrosol and the homovanillic alcohol were subjected to chemoselective lipase-catalyzed acylations, affording with good yield of 10 derivatives bearing C_2, C_3, C_4, C_{10}, and C_{18} acyl chains at C-1. The hydroxytyrosol

* Corresponding author. Prof. Youssef Gargouri, Laboratoire de Biochimie et de Génie Enzymatique des Lipases, ENIS route de Soukra, 3038 Sfax-Tunisia., Tel/ Fax: + 21674675055, E-mail: ytgargouri@yahoo.fr.

[†] Laboratoire de Biochimie et de Génie Enzymatique des Lipases.

[‡] Laboratoire des Bioprocédés.

[§] Laboratoire de Chimie Industrielle II.

10.1021/jf071685q CCC: $37.00 © 2007 American Chemical Society
Published on Web 11/15/2007

and its lipophilic derivatives with little hydrophobic character showed a good protective effect against H_2O_2-induced oxidative DNA damage (*20*) and very good DPPH-radical scavenging activity (*21*). Furthermore, it was reported that the acetylated derivatives of tyrosol were more potent inhibitors of PAF-induced rabbit platelet aggregation than tyrosol, indicating that the addition of an acetyl group on the tyrosol structure results in phenolic compounds that are more potent inhibitors by 2 orders of magnitude (*22*).

The present work focuses on the reaction parameters that affect the enzymatic acetylation of tyrosol with ethyl acetate by an immobilized *Staphylococcus xylosus* lipase. In addition, the aim of this study was to determine, by means of response surface methodology (RSM), the optimal conditions of tyrosol acetate ester synthesis. A Box Behnken design (*23–25*) is set up to establish the relationship between the conversion yield of tyrosol acetate and the reaction factors (ethyl acetate/hexane volume ratio, enzyme amount, and temperature). The enzymatic synthesis yields were compared to the chemical methods.

MATERIALS AND METHODS

Materials. The tyrosol, the deuterated chloroform ($CDCl_3$), and the 2,2-diphenyl-1-picrylhydrazyle (DPPH) were purchased from Fluka (Suisse). The *n*-hexane, the acetone, the pyridine, and the acyl chlorure were purchased from Prolabo (Paris, France).The carbonate of calcium ($CaCO_3$) and the ethyl acetate were purchased from Pharmacia (Uppsala, Sweden).

Instrumentation. *HPLC Analysis.* The identification of tyrosol and its acetylated derivatives was carried out by HPLC analysis. It was performed on a Shimadzu apparatus composed of an LC-10ATvp pump and an SPD-10Avp detector. The column was a C-18 (4.6 × 250 mm; Shimpack VP-ODS), and its temperature was maintained at 40 °C. The flow rate was 0.5 mL/min. The mobile phase used was 0.1% phosphoric acid in water (A) versus 70% acetonitrile in water (B) for a total running time of 50 min, and the following proportions of solvent B were used for the elution: 0–30 min, 20–50%; 30–35 min, 50%; and 35–50 min, 50–20%.

LC–MS Analysis. The LC–MS experiments were carried out with an Agilent 1100 LC system consisting of degasser, binary pump, autosampler, and column heater. The column outlet was coupled to an Agilent MSD Ion Trap XCT mass spectrometer equipped with an ESI ion source. Data acquisition and mass spectrometric evaluation were carried out on a personal computer with *Data Analysis* software (Chemstations). For the chromatographic separation, a Zorbax 300 Å Extend-C-18 column (2.1 × 150 mm) was used. The column was held at 95% solvent A (0.1% formic acid in water) and 5% solvent B (0.1% formic acid in ACN) for 1 min, followed by an 11 min step gradient from 5% B to 100% B; then, it was kept for 4 min with 100% B; finally, the elution was achieved with a linear gradient from 100% B to 5% B in 2 min. The flow rate was 200 μL $min^{-1,}$ and the injection volume 5 μL.

NMR and IR Experiments. NMR spectra were recorded on JNM A-300 spectrometer (JEOL). IR spectra were recorded on FT/IR-410 (JASCO).

Production and Immobilization of Lipase. *Staphylococcus xylosus* lipase was produced as described by Mosbah et al. (*26*). The enzyme immobilization was made onto $CaCO_3$ as described by Ghamgui et al. (*27*). The activities of the immobilized lipases were measured titrimetrically with a pH-stat, under the standard assay conditions described previously by Gargouri et al. (*28*) using olive oil emulsion as the substrate. One international unit (UI) of lipase activity was defined as the amount of lipase that catalyzes the liberation of 1 μmol of fatty acid from olive oil per minute at pH 8.5 and 37 °C.

Alcoholysis Reactions. The transesterification reactions were carried out in screw-capped flasks containing 12 mM tyrosol added to various ethyl acetate to *n*-hexane volume ratios (6 mL of total volume), followed by different amounts of immobilized lipase. The mixture reaction was incubated at different temperatures with shaking (200 rpm). A reaction under the same conditions without adding enzyme was realized in parallel. After 48 h of reaction, aliquots of the mixture reaction were withdrawn; the immobilized enzyme was removed by centrifugation at 8000 rpm for 5 min, and the supernatant was used for HPLC analysis. A calibration curve based on different concentrations of tyrosol was employed using benzoic acid as the internal standard. The conversion yield of tyrosol acetate was calculated as the ratio of the number of moles of tyrosol used per total number of tyrosol.

Table 1. Three-Variable Box-Behnken Experimental Design

run	X_1	X_2	X_3
1	−1.0000	−1.0000	0.0000
2	1.0000	−1.0000	0.0000
3	−1.0000	1.0000	0.0000
4	1.0000	1.0000	0.0000
5	−1.0000	0.0000	−1.0000
6	1.0000	0.0000	−1.0000
7	−1.0000	0.0000	1.0000
8	1.0000	0.0000	1.0000
9	0.0000	−1.0000	−1.0000
10	0.0000	1.0000	−1.0000
11	0.0000	−1.0000	1.0000
12	0.0000	1.0000	1.0000
13	0.0000	0.0000	0.0000

Tyrosol (1). Colorless amorphous solid. MS: mass calculated 138 for $C_8H_{10}O_2$ found *m/z* 161 $[M + Na]^+$, 120 $[M - H_2O]^+$, 93[M-CH_2-CH_2-OH]$^+$. IR (liquid) cm^{-1}: 3323 (m), 1590 (s). ^{1}H NMR (300 MHz, $CDCl_3$): 7.1 (2H, d, $J = 8$ Hz), 6.8 (2H, d, $J = 8$ Hz), 4.8 (1H, s,-OH), 3.8 (2H, t, $J = 7$ Hz, -CH_2C<u>H</u>$_2$OH), 2.8 (2H, t, $J = 7$ Hz, -C<u>H</u>$_2$$CH_2$OH), 1.6 (1H, s,-O<u>H</u>). ^{13}C NMR (75 MHz, $CDCl_3$): 38.62 (C-7), 64,24 (C-8), 115.84 (C-3, C-5), 130.57 (C-2, C-6), 130.81 (C-1), 154.64 (C-4).

Monoacetylated Tyrosol (2). Colorless oil. After 48 h of incubation, the monoacetylated tyrosol was purified by preparative HPLC under the same conditions as the analytic one. LC-MS analysis showed a fragment at *m/z* 181 $[M + H]^+$, 202, 7 $[M + Na]^+$; 120 $[M - H_2O]^+$, 93 [M-CH_2-CH_2-OH]$^+$ ([M]$^+$, calculated for 180, 2004 $C_{10}H_{12}O_3$). IR (liquid) cm^{-1}: 3323 (m), 1726 (m), 1620 (m), 1250 (s). ^{1}H NMR (300 MHz, $CDCl_3$): 7.1 (2H, d, 7.8 Hz), 6.8 (2H, d, 7.8 Hz), 2.06 (3H, s, $COCH_3$), 4.2 (2H, t, 2.7 Hz, -CH_2-C<u>H</u>$_2$-**O**$COCH_3$), 2.8 (2H, t, 2,7 Hz,-C<u>H</u>$_2$-CH_2-$COCH_3$), 1.26 (1H, s, -O<u>H</u>). ^{13}C NMR (75 MHz, $CDCl_3$): 21.1 (C-10), 34.1 (C-7), 65.6 (C-8), 115.84 (C-3, C-5), 130.1 (C-2, C-6), 129.4 (C-1), 154.6 (C-4), 172.1 (C-9, C=O).

Diacetylated Tyrosol (3). Colorless oil; after 1 h of incubation, the diacetylated tyrosol was purified by preparative HPLC under the same conditions as the analytic one. LC-MS analysis showed a fragment at *m/z* 223 $[M + H]^+$, 245 $[M + Na]^+$, ([M]$^+$, calculated for 222, 2371 $C_{12}H_{14}O_4$).

Experimental Design. Optimization of the experimental conditions of the synthesis of a phenolic acid ester was achieved by using response surface methodology (RSM). Recall that RSM is a technique consisting of (i) design of experiment to provide adequate and reliable measurements of the response, (ii) development a mathematical model having the best fit to the data obtained from the experimental design, and (iii) determination of the optimal values of the independent variables that produce maximum or minimum value of the response (*23–25*).

In this paper, RSM was applied to establish and exploit the relationship between the response studied (conversion yield of the tyrosol acetate) and the three selected experimental variables (ethyl acetate/hexane volume ratio, enzyme amount, and temperature). In this regard, we have postulated a quadratic polynomial model represented by the following equation:

$$\hat{y} = b_0 + b_1X_1 + b_2X_2 + b_3X_3 + b_{11}X_1^2 + b_{22}X_2^2 + b_{33}X_3^2 + b_{12}X_1X_2 + b_{13}X_1X_3 + b_{23}X_2X_3 \quad (1)$$

with $y = \hat{y} + e$, where e represents deviation between measured response (y) and estimated response ($\hat{y}$); b_0, b_j, b_{jk}, and b_{jj} are estimated model coefficients; and X_j represents coded variables related to the corresponding natural variable U_j by the equation $X_j = (U_{j\ \mathrm{high}}$ and $U_{j\ \mathrm{low}} =$ high and low levels of U_j).

Table 2. Range of Variables for the Experimental Design

variable	level −1	0	+1
U_1: ethyl acetate/hexane volume ratio (v/v)	0.20	0.60	1.00
U_2: enzyme amount (UI)	50	275	500
U_3: temperature (°C)	40	50	60

To estimate the model coefficients, a three-variable Box Behnken design, requiring 13 experiments (**Table 1**), is carried out in a cubic experimental domain. The experimental points are located in the middle of a cube ridges (12 experiments) and at the center of the cube (1 experiment) (*23–25*). The model parameters are estimated by a least-squares fitting of the model to experimental results obtained in the design points. The adequacy of the model is tested using four check points (*24, 25*).

The fitted model is used to study the relative sensitivity of the response to the variables and to look for the optimal experimental conditions. In this paper, the relationship between the response and the experimental variables is illustrated graphically by plotting the response surfaces and the isoresponse curves (*23*). The canonical analysis is used to determine the best experimental conditions, which permitted the maximization of the yield conversion of the tyrosol acetate synthesis yield. It consists of rewriting the fitted second-degree equation in a form in which it can be more readily understood. This is accomplished by a rotation of axes that remove all cross-product terms b_{jk}, X_j, and X_k, while keeping the initial origin at the center point. This step is suitable when the stationary point is outside the experimental domain.

In this study, the generation and the data treatment of the Box-Behnken design are performed using the experimental design software *NemrodW* (*29*).

DPPH Radical-Scavenging Effect. The DPPH radical-scavenging effect was evaluated according to Bouaziz et al. (*30*). A 4 mL volume of methanolic solution of varying sample concentration was added to 10 mL of DPPH methanol solution (0.15 mM). After mixing the two solutions gently and leaving for 30 min at room temperature, the optical density was measured at 520 nm, using a spectrophotometer. The antioxidant activity of each sample was expressed in terms of IC_{50} (micrograms per milliliter required to inhibit DPPH radical formation by 50%) and calculated from the log-dose inhibition cuve.

Chemical Synthesis of Acetylated Tyrosol. Acetylation was generated by a modified method according to Capasso et al. (*31*). Briefly, acetic anhydride (160 μL) was added to tyrosol (0.145 mmol). The reaction was left at 0 °C overnight. After that, 150 μL of sulfuric acid were added and kept for 4 h at 0 °C. The reaction mixture was treated to neutrality with $NaHCO_3$, and the ester was extracted by ethyl acetate. Acetylated derivatives was concentrated *in vacuo* to dryness at 40 °C, dissolved in ethyl acetate, and analyzed by HPLC and LC-MS.

RESULTS AND DISCUSSION

To prepare the acetylated derivative of tyrosol, immobilized *Staphylococcus xylosus* lipase was used. Several conditions were tested, including different amounts of enzyme, various temperatures, and ethyl acetate/hexane volume ratio. In a preliminary study, we showed that the addition of hexane to the reaction medium was necessary to improve the stability of the immobilized *Staphylococcus xylosus* lipase. Also, we found that the addition of water at the beginning of the reaction or a crude molecular sieve 4 Å (5%, w/w) failed to improve the conversion yield. In light of these results, the ethyl acetate/hexane volume ratio (U_1), the amount of enzyme (U_2), and the temperature (U_3) are chosen as the most effective operating variables on the response.

Experimental Design Data. To carry out the Box-Behnken experimental design, a high and a low level were chosen for each factor (**Table 2**). **Table 3** shows the real experimental conditions of the Box-Behnken design with the corresponding measured responses. Four additional experiments (runs no 14 to 17) are included in order to check the validity of the fitted model.

Table 3. Experimental Conditions of the Box-Behnken Design and the Corresponding Experimental Responses

run	ethyl acetate/hexane	enzyme (UI)	temperature (°C)	yield[a]%
1	0.20	50	50	77.07
2	1.00	50	50	65.12
3	0.20	500	50	94.79
4	1.00	500	50	83.39
5	0.20	275	40	74.12
6	1.00	275	40	59.69
7	0.20	275	60	77.22
8	1.00	275	60	62.79
9	0.60	50	40	62.20
10	0.60	500	40	67.66
11	0.60	50	60	41.40
12	0.60	500	60	80.00
13	0.60	275	50	83.55
14	0.60	250	50	80.71
15	0.50	500	40	74.00
16	0.60	400	60	79.53
17	0.66	500	50	82.11

[a] Estimated standard deviation is equal to SD = ✓(38.80/3) = 3.60.

Table 4. Analysis of Variance

source of variation	sum of squares	degrees of freedom	mean square	*F*-ratio	prob > *F*	signif
regression	2196.33	9	244.036	18.869	1.71	*[a]
residuals	38.80	3	12.933			
total	2235.13	12				
R^2	0.983					

[a] * indicates significant at the level 95%.

Table 5. Validation of the Model with the Check-Points

run	y_i	$\hat{y}_i$	$e = y_i - \hat{y}_i$	*t* exp.	signifiance
14	80.71	82.382	−1.672	−0.330	N.S.
15	74	66.484	7.516	1.569	N.S.
16	79.53	75.84	3.69	0.830	N.S.
17	82.11	88.074	−5.964	−1.329	N.S.

Estimated Models. The observed responses (runs 1 to 13) are used to compute the model coefficients by the least-squares method (*23, 24*) using the *NemrodW* software. The resulting estimated model, expressed in coded variables, is

$$\hat{y} = 83.55\ (\pm 3.60) - 6.53\ (\pm 1.27)X_1 + 10.01\ (\pm 1.27)X_2 - 0.28\ (\pm 1.27)X_3 + 1.09\ (\pm 2.38)X_1^2 - 4.55\ (\pm 2.38)X_2^2 - 16.19\ (\pm 2.38)X_3^2 + 0.14\ (\pm 1.80)X_1X_2 + 0.00\ (\pm 1.80)X_1X_3 + 8.29\ (\pm 1.80)X_2X_3$$

Analysis of Variance and Validation of the Models. The fit quality of the yield model is attested with analysis of the variance (ANOVA) as revealed in **Table 4**. Indeed, this table shows that the regression sum of squares is statistically significant when using the *F*-test at a 95% probability level, which suggested that the variation accounted for by the model was significantly greater than the unexplained variation. Likewise, the fit value, the coefficient of multiple determination of the polynomial model, termed R^2, was equal to 0.983, which indicated that 98.3% of the variability in the response could be explained by the second-order polynomial prediction equation given above. On the other hand, we used the four check-point results to validate the fitted model. It can be seen, from **Table 5**, that the measured values y_i are very close to those calculated

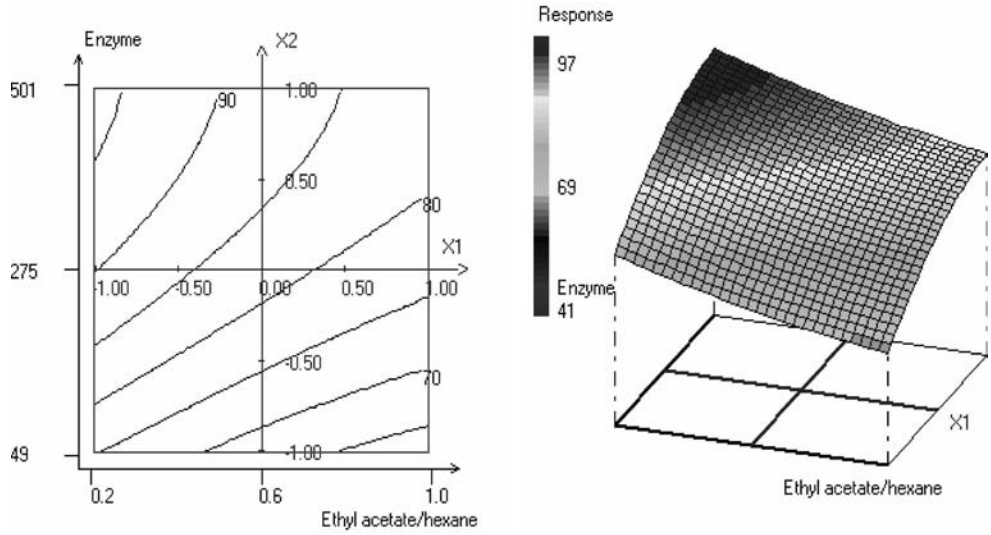

Figure 1. Contour plots and response surface plot showing the effect of enzyme amount, ethyl acetate /hexane volume ratio, and their mutual interaction on tyrosol acetate synthesis at constant temperature equal to 50 °C.

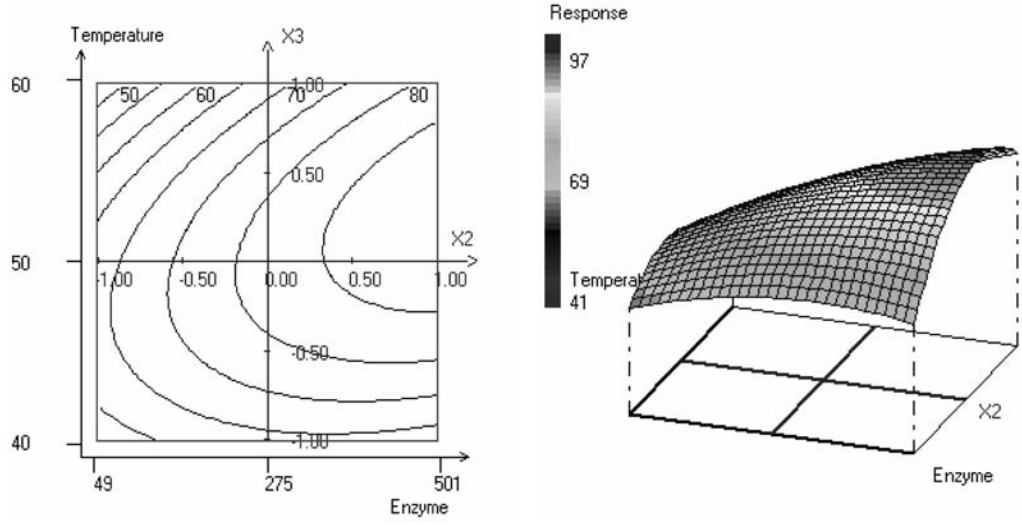

Figure 2. Contour plots and response surface plot showing the effect of enzyme amount, temperature, and their mutual interaction on tyrosol acetate synthesis at ethyl acetate/hexane volume ratio fixed at 0.6.

($\hat{y}_i$) using the model equation. Besides, the differences between calculated and measured responses are not statistically significant when using the *t* test at a 95% probability level. We can then conclude that the second-order model is adequate to describe the response surfaces, and it can be used as a prediction equation in the studied domain.

Graphical Interpretation of the Response Surface Model. Following the validation of the model, the response surface and the isoresponse curves are drawn by plotting the response variation against two of the factors while the third is held constant at its mean level.

Figure 1 shows the effect of enzyme amount (50–500 UI) and ethyl acetate/hexane volume ratio (0.2–1) on the conversion yield of tyrosol acetate at 50 °C.We have observed that the conversion yield enhances essentially by increasing the amount of enzyme or lowering the ethyl acetate/hexane volume ratio. Indeed, the contour plots in **Figure 1** show that a high tyrosol acetate synthesis yield (95%) can be obtained by using a high amount of enzyme (over 400 UI) and low ethyl acetate/hexane volume ratio (under 0.3). This result can be explained by the negative effect of the solvent ratio on the enzyme activity, which greatly affects the reaction yield. These data agree with those of Klibanov (*32*), who stated that the enzyme activity is strongly affected by the choice of organic solvent. In fact, the use of hydrophilic solvents with log $P < 2.5$ have the capability of stripping off even the essential water from the enzyme surface, leading to an insufficiently hydrated enzyme molecule and consequently to a decrease of the enzyme activity (*33*). The solvents with log $P > 4$ show better reaction rates. Therefore, the hydrophobic solvents preserve the catalytic activity without disturbing the microaqueous layer of the enzyme.

Figure 2 shows the effect of varying the enzyme amount (50–500 UI) and the reaction temperature (40–60 °C) on alcoholysis at a constant solvent volume ratio ($U_1 = 0.6$). It can be seen that, at low enzyme amount and temperature, the conversion yield was strongly decreased, whereas high reaction yields were obtained when using high enzyme level and moderate temperature. In fact, high temperature (above 55 °C) dramatically decreased the conversion yield at any given enzyme amount. This phenomenon is probably due to the inactivation of the enzyme at high temperature. Krishna et al. (*34*) suggested that high temperature can reduce the operational stability of the enzyme. Chiang et al. (*35*) had observed that an increase of the temperature up to 55 °C resulted in a lower alcoholysis yield at

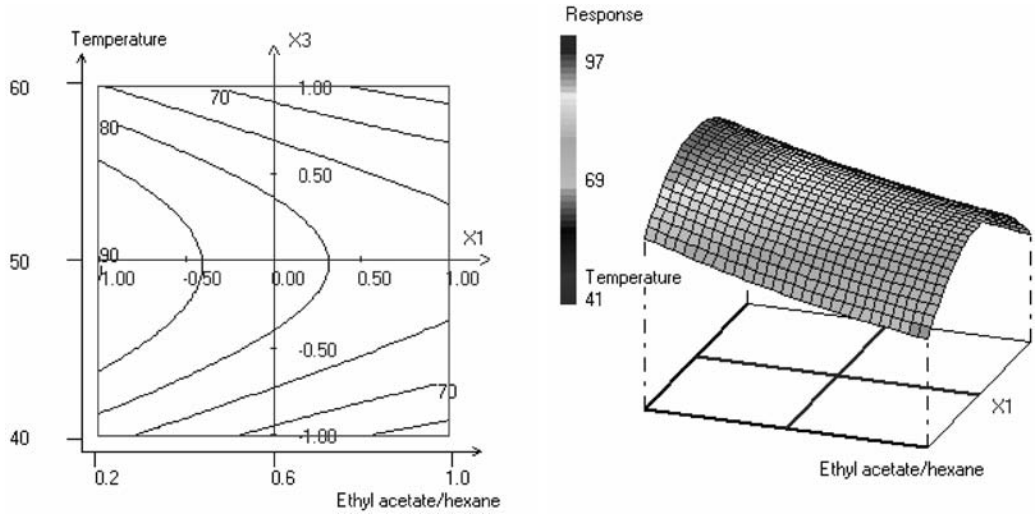

Figure 3. Contour plots and response surface plot showing the effect of ethyl acetate /hexane volume ratio, temperature, and their mutual interaction on tyrosol acetate synthesis with enzyme amount fixed at 0.6.

any given amount of enzyme because of the inactivation of the lipase at high temperatures. We can also conclude, from this figure, that the reaction conducted with a high amount of enzyme (over 300 UI) at 50 °C led to a relatively high conversion yield (85%). However, with an amount of lipase higher than 500 UI, the difference almost leveled off (data not shown). The amount of enzyme is probably the rate-determining factor of the reaction up to 500 UI. This phenomenon may be related to the fact that the active sites of the enzyme molecules present in large excess would not be exposed to the substrates due to possible protein aggregation. As a result, lipase molecules can associate with each other, masking the active sites that cannot accommodate the substrate. Agglomeration using immobilized lipases has been reported by Foresti and Ferreira 36. **Figure 3** shows the variation of the reaction yield in the plane solvent volume ratio (0.2–1) versus temperature (40–60 °C) at a constant level of enzyme (500 UI). This figure confirms the negative effect of the ethyl acetate /hexane volume ratio on the tyrosol acetate yield already shown in **Figure 1**. It also illustrates that, at constant enzyme level, the tyrosol acetate synthesis carried out at a moderate reaction temperature (approximately 50 °C) and the lowest solvent volume ratio (0.2) gave a high conversion yield (90%). To further analyze the experimental results and to obtain a more precise estimation of the optimum synthesis conditions, we applied the canonical analysis.

Canonical Analysis. The second-order polynomial model is a conic function and it can be analyzed by canonical analysis. This function has a stationary point *S* where the partial derivative of predicted response with respect to each of the variables is zero $\partial y / \partial X_1 = 0; \partial y / \partial X_2 = 0; \partial y / \partial X_3 = 0$. This point could be a maximum, a minimum, or a saddle point.

In the present study, the coordinates of the stationary point *S* are $X_1 = 2.721$; $X_2 = 1.505$; and $X_3 = 0.419$. It corresponds to a maximum of $\hat{y}$. This point is situated outside the experimental domain at a distance from the center equal to 3.14. In this case, the canonical analysis requires only a rotation of the X_j axes in such a way that they become parallel to the principal axes Z_j of the contour system. Under these conditions, the canonical model is of the form

$$\hat{y} = y_s + \sum_{j=1}^{3} b_j Z_j + \sum_{j=1}^{3} \lambda_{jj} Z_j^2 \qquad (2)$$

The λ_j ($i = 1, 2, 3$) will describe the curvature of the response, while the linear coefficient b_j will describe the slope of the ridge

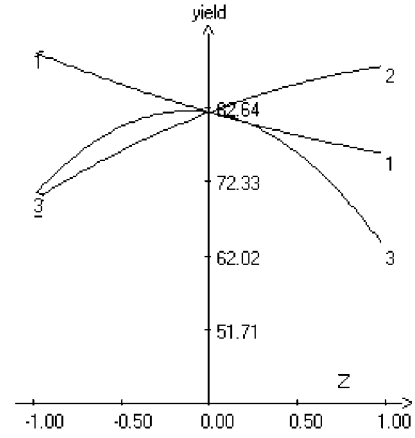

Figure 4. Curvature of yield response versus Z_j.

in the corresponding direction. The constant y_s is the calculated response value at the stationary point. The interpretation is easier by analyzing each response along every Z_j-axis separately. Using the variable transformation equations (not shown), we obtained the following canonical form of the model:

$$\hat{y} = 82.011 - 7.088Z_1 + 9.339Z_2 - 3.657Z_3 + 1.325Z_1^2 - 2.853Z_2^2 - 15.218Z_3^2 \qquad (3)$$

These data allow us to determine the features of the response surface in each direction of the experimental domain. When analyzing the response surface along each of the three directions OZ_1, OZ_2, and OZ_3, the equation of the response is reduced to the following equations, respectively:

$$\hat{y} = 82.011 - 7.088Z_1 + 1.325Z_1^2 \qquad (4)$$

$$\hat{y} = 82.011 + 9.339Z_2 - 2.853Z_2^2 \qquad (5)$$

$$\hat{y} = 82.011 - 3.657Z_3 - 15.218Z_3^2 \qquad (6)$$

The corresponding curves are represented in **Figure 4**. From these curves and the variable transformation equations, we can conclude that the maximization of the yield requires a low level of X_1 ($X_1 = -1$), a high level of X_2 ($X_2 = +1$), and the mean level of X_3 ($X_3 = 0$). This corresponds to the following settings of the natural variables: ethyl acetate/hexane volume ratio $U_1 = 0.2$; enzyme amount $U_2 = 500$ UI; and temperature U_3 in

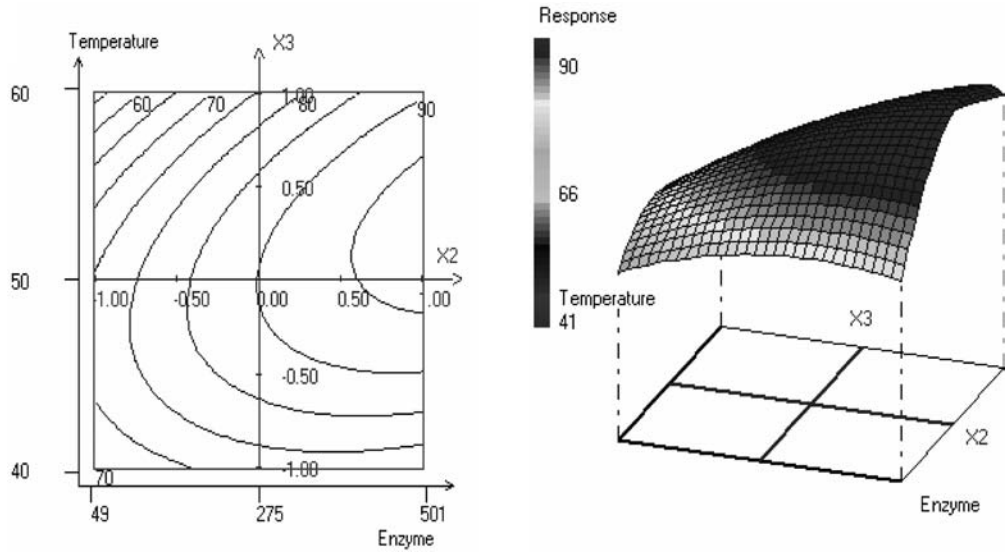

Figure 5. Contour plots and response surface plot showing the effect of enzyme amount, temperature, and their mutual interaction on tyrosol acetate synthesis at ethyl acetate/hexane volume ratio fixed at 0.6.

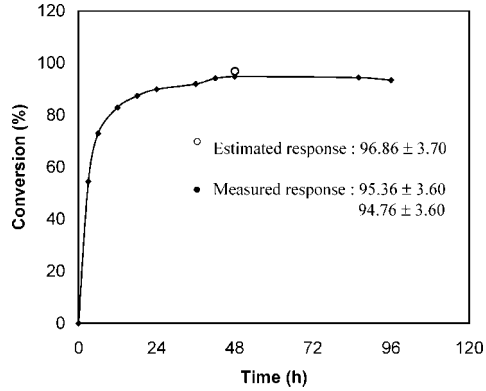

Figure 6. Production of tyrosol acetate during alcoholysis reaction. Reaction conditions: ethyl acetate/hexane volume ratio of 0.2, 500 UI enzyme amount, and temperature of 54 °C. The tyrosol acetate level was estimated using the HPLC system.

the vicinity of 50 °C. As the results of the canonical analysis agree with those of the contour plot study, we can conclude that there is no a masked optimum: the one predicted by a few sections of contour plot analysis represents a real optimum for the whole experimental domain.

Result Confirmation. In order to confirm the obtained result, two independent replicates were carried out under the following conditions: ethyl acetate/hexane volume ratio equal to 0.2; enzyme amount equal to 500 UI; and temperature equal to 54 °C. The temperature value is indicated by the contour plots represented in **Figure 5** and generated from the fitted model by keeping constant the solvent mixture ratio ($U_1 = 0.2$). These contour plots indicated that, under these conditions, the predicted conversion yield was 96.86%. Moreover, we showed how sensitive the estimated response is to movements away from the optimum. The conversion yields obtained at 48 h of reaction time are indicated in **Figure 6**, together with the value calculated from the model equation. These results clearly showed that the experimental response values agree with those calculated. Once again, this verification revealed a high degree of accuracy of the model under the investigated conditions.

The time course of the alcoholysis reaction between the tyrosol and the ethyl acetate by immobilized *S. xylosus* lipase onto $CaCO_3$ under optimal conditions (acetate/hexane volume ratio of 0.2; 500 UI enzyme amount, and temperature of 54 °C) was presented in **Figure 6**. The level of tyrosol acetate increases rapidly to reach its maximal value after 48 h. The experimental conversion yield of tyrosol acetate (95.36%) was very close to the predicted value estimated (96.86 ± 3.70) after a reaction time of 48 h.

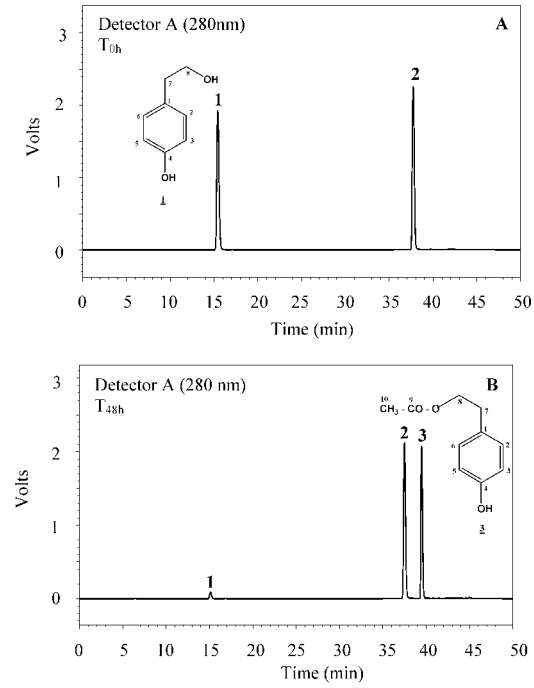

Figure 7. HPLC chromatogram of the reaction medium in the optimal conditions. The separation was made on C18 reverse-phase HPLC. Flow 0.6 mL/min, and UV detection was at 280 nm. **A**. Time = 0. **B**. Time = 48 h. **1**. Tyrosol. **2**. Internal standard. **3**: Monoacetyltyrosol.

Structure Determination of Enzymatic Acetylated Derivative. Tyrosol contains two hydroxyl groups in its structure, and therefore three acetylated derivatives were expected: two isomers with two monoacetylated derivatives and one diacetylated derivative. HPLC analysis of the reaction mixture after 48 h (**Figure 7**) showed a new peak which corresponds to the acetylated derivative. The purified compound was characterized by spectroscopic methods.

To establish the structure of acetylated derivatives, a positive mass spectrum was performed. Standard tyrosol gave two peaks

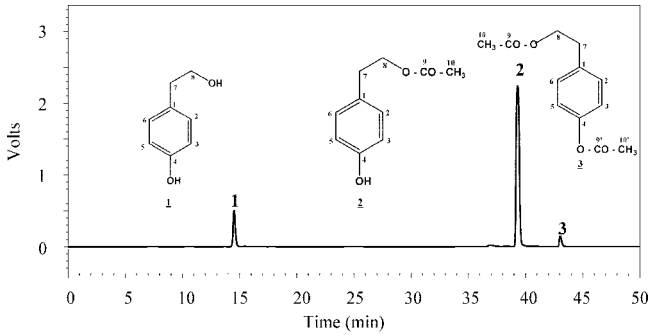

Figure 8. HPLC chromatogram of the reaction medium of the chemical acetylation of tyrosol. The separation was made on C18 reverse-phase HPLC. Flow was 0.6 mL/min, and UV detection was at 280 nm. **1**. Tyrosol. **2**. Monoacetyltyrosol. **3**. Diacetylhydroxytyrosol.

at *m/z* 121 $[M - H_2O]^+$ and 161 $[M + Na]^+$. The acetylated derivative showed almost identical positive mass spectrum as its native form. The predominant peaks were at *m/z* 203 $[M + Na^+]$ and 181 which corresponds to the molecular weight of a tyrosol molecule plus an acetyl group. In order to locate the position of the acetylation, IR and NMR experiments were carried out. IR spectra showed a broad band at around 3323 cm^{-1} corresponding to characteristic hydrogen-bonded phenolic O–H vibration and a characteristic band at around 1726 cm^{-1} attributed to the ester function C═O. These data provide evidence of the existence of acetyl groups in the molecule and the perseverance of the hydroxyl group. The presence of an acyl group linked to the tyrosol and its position were determined by comparison of ^1H NMR and ^{13}C NMR spectra between the acetylated tyrosol and its native form. With regard to ^{13}C NMR data, the spectrum of the acetylated tyrosol showed signals at δ 172 ppm and δ 21, 1 ppm, which were attributed to a carbon ester function (C-9) and the methyl function (C-10), respectively (**Figure 7**). By ^1H NMR, we were able to locate the position of the acetylated hydroxyl. Data showed a chemical shift of triplet ^2H at 4.2 ppm attributed to the protons of carbon C8 for the acetylated derivative, whereas the chemical shift of the same protons in the native form was detected at 3.8 ppm, suggesting that the acetyl group was linked to the methylene group (C8). For the aromatic protons of the tyrosol and its monoacetylated form, no modification of chemical shift was observed. These results led to the conclusion that the tyrosol was monoacetylated on the primary hydroxyl group. Similar results have been reported by Grasso et al. (*20*) during the chemical acetylation of hydroxytyrosol by fatty acids. However, to our knowledge, no reports on the enzymatic acetylation of tyrosol have been reported.

Chemical Acetylation. A mixture composed of acetic acid anhydride and sulfuric acid or pyridine represents the usual acetylating agents, described in many studies for the acetylation of polyphenols (*31*). HPLC analysis (**Figure 8**) of the reaction mixture showed two peaks attributed to acetylated derivatives. Under the above conditions, a conversion yield of 94.08% was obtained. To establish the structures of the synthesis products, LC-MS analysis was performed. The positive ion mass spectrum of peak 2 gave an identical positive mass spectrum to that of the monoacetylated tyrosol obtained by the enzymatic method, indicating that the predominant peak 2 corresponds to the monoacetylated tyrosol. The positive ion mass spectrum of peak 3 gave molecular peaks at *m/z* 223 $[M + H]^+$ as well as at *m/z* 245 $[M + Na]^+$, corresponding to the molecular weight of tyrosol plus two acetyl groups corresponding to the molecular weight of tyrosol plus two acetyl groups. These data in combination with results obtained for monoacetylated tyrosol lead to the conclusion that peak 3 is the diacetyl derivative of tyrosol. This compound has previously been chemically synthesized and identified by the use of ESI-MS in the negative mode (*22*).

DPPH Radical Scavenging Effect of Tyrosol and Monoacetylated Tyrosol. The DPPH (2,2 diphenyl-2-picrylhydrazyl) radical scavenging effect of both tyrosol and monoacetylated tyrosol was measured and compared to that of BHT (1 μg/mL). Tyrosol exhibited IC_{50} values of 10.9 μg/mL and in the same ring compared to that of monoacetylated tyrosol (10.25 μg/mL). These findings suggest that the scavenging activity of tyrosol is not notably influenced by the presence of an acyl group. It has been reported that the antioxidant activity was related to the number and nature of the hydroxylation pattern on the aromatic ring. It is generally assumed that the ability to act as a hydrogen donor and the inhibition of oxidation are enhanced by increasing the number of hydroxyl groups in the phenol ring (*30*). Other results are in line with our findings and show that the antiradical activity of hydroxytyrosol was not affected by the presence of an acyl group at C-1 (*20*). In addition, Fragopoulou et al. (*22*) reported that the monoacetylated derivatives of tyrosol were more potent inhibitors of PAF-induced rabbit platelet aggregation than tyrosol. Meanwhile, the diacetylated derivative induced washed rabbit platelet aggregation and inverted the biological activity from inhibition to aggregation.

In this study, the evaluation of the effect of the ethyl acetate/hexane volume ratio (0.2–1), enzyme amount (50–500 UI), and temperature (40–60 °C) on acetylated tyrosol yield was studied. The optimization of synthesis conditions was performed using response surface methodology. A Box-Behnken design permits determination of the optimal conditions (reaction temperature of 54 °C, enzyme amount of 500 UI, and volume ratio of ethyl acetate/hexane of 0.2) leading to a high conversion yield (95.3%). The product obtained under these conditions was identified, using spectroscopic methods, to be a monoacetylated derivative of tyrosol which exhibited the same radical scavenging activity as tyrosol. Chemical acetylation produced mono- and diacetylated tyrosol, which provides evidence of the chemoselective properties of the biocatalyzed acetylation. The existence of lipophilic derivatives of phenols via esterification of the hydroxyl functions with aliphatic molecules can be used as a tool to increase their lipophilicity and therefore improve their intestinal absorption and cell permeability. Moreover, this lipophilic analogue could be used as food antioxidant in oil-based formulae or cosmetic fields.

ABBREVIATIONS USED

SXL: *Staphylococcus xylosus* lipase; SXL_i, immobilized *Staphylococcus xylosus* lipase; UI, enzymatic international unit; $CaCO_3$, calcium carbonate; $CDCl_3$, deuterated chloroform; HPLC, high performance liquid chromatography; LC-MS, high performance liquid chromatography coupled to mass spectrometry; IR, infrared; NMR, nuclear magnetic resonance; DPPH, 2,2-diphenyl-1-picrylhydrazyle.

ACKNOWLEDGMENT

We are grateful to Mr. A. Gargoubi (technician, CBS), Mr. H. Auissaoui (engineer, CBS), Mrs. E. Dabbabi (engineer, FSM), and Mrs. A. Kbadou (assistant professor, FSS) for their technical assistance. Our thanks are due to LPRAI - Marseille Company for supplying us with the software package *NemrodW*.

LITERATURE CITED

(1) Heim, K. E.; Tagliaferro, A. R.; Bobilya, D. J. Flavonoid antioxidants: chemistry, metabolism and structure-activity relationships. *J. Nutr. Biochem.* **2002**, *13*, 572–584.

(2) Di Carlo, G.; Mascolo, N.; Izzo, A. A.; Capasso, F. Flavonoids: old and new aspects of a class of natural therapeutic drugs. *Life Sci.* **1999**, *65*, 337–353.

(3) Tuck, K. L.; Hayball, P. J. Major phenolic compound in olive oil: metabolism and health effects. *J. Nutr. Biochem.* **2002**, *13*, 636–644.

(4) Fki, I.; Allouche, N.; Sayadi, S. The use of polyphenolic extract, purified hydroxytyrosol and 3,4-dihydroxyphenyl acetic acid from olive mill wastewater for the stabilization of refined oils: a potential alternative to synthetic antioxidants. *Food Chem.* **2005**, *93*, 197–204.

(5) De la Puerta, R.; Martinez Dominguez, M. E.; Ruiz-Gutierrez, V.; Flavill, J. A.; Hoult, J. R. Effects of virgin olive oil phenolics on scavenging of reactive nitrogen species and upon nitrergic neurotransmission. *Life Sci.* **2001**, *69*, 1213–1222.

(6) Bertelli, A. A.; Migliori, M.; Panichi, V.; Longoni, B.; Origlia, N.; Ferretti, A.; Cuttano, M. G.; Giovannini, L. Oxidative stress and inflammatory reaction modulation by white wine. *Ann. N. Y. Acad. Sci.* **2002**, *957*, 295–301.

(7) Giovannini, L.; Migliori, M.; Filippi, C.; Origlia, N.; Panichi, V.; Falchi, M.; Bertelli, A. A.; Bertelli, A. Inhibitory activity of the white wine compounds, tyrosol and caffeic acid, on lipopolysaccharide-induced tumor necrosis factor-alpha release in human peripheral blood mononuclear cells. *Int. J. Tissue React.* **2002**, *24*, 53–56.

(8) De la Puerta, R.; Ruiz-Gutierrez, V.; Hoult, J. R. Inhibition of leukocyte 5-lipoxygenase by phenolics from virgin olive oil. *Biochem. Pharmacol.* **1999**, *57*, 445–449.

(9) Giovannini, L.; Migliori, M.; Filippi, C.; Origlia, N.; Panichi, V.; Falchi, M.; Bertelli, A. A.; Bertelli, A. Inhibitory activity of the white wine compounds, tyrosol and caffeic acid, on lipopolysaccharide- induced tumor necrosis factor-R release in human peripheral blood mononuclear cells. *Int. J. Tissue React.* **2002**, *24*, 53–56.

(10) Giovannini, C.; Straface, E.; Modesti, D.; Coni, E.; Cantafora, A.; De Vincenzi. ; Malorni, W.; Masella, R. Tyrosol, the major olive oil biophenol, protects against oxidized LDL-induced injury in Caco2 cells. *J. Nutr.* **1999**, *129*, 1269–1277.

(11) Bu, Y.; Rho, S.; Kim, J.; Kim, M. Y.; Lee, D. H.; Kim, S. Y.; Choi, H.; Kim, H. Neuroprotective effect of tyrosol on transient focal cerebral ischemia in rats. *Neurosci. Lett.* **2007**, *414*, 218–221.

(12) Di Benedetto, R.; Varı, R.; Scazzocchio, B. ; Filesi, C.; Santangelo, C.; Giovannini, C.; Matarrese, P.; D'Archivio, M.; Masella, R. Tyrosol, the major extra virgin olive oil compound, restored intracellular antioxidant defences in spite of its weak antioxidative effectiveness. *Nutrition, Metabolism & Cardiovascular Diseases* 2007, *7*, 535–545.

(13) Katiyar, S. K.; Elmets, C. A. Green tea polyphenolic antioxidants and skin photoprotection. *Int. J. Oncol.* **2001**, *18*, 1307–1313.

(14) Lupo, M. P. Antioxidants and vitamins in cosmetics. *Clin. Dermatol.* **2001**, *19*, 467–473.

(15) Suda, I.; Oki, T.; Masuda, M.; Nishiba, Y.; Furuta, S.; Matsugano, K.; Sugita, K.; Terahara, N. Direct absorption of acylated anthocyanin in purple-fleshed sweet potato into rats. *J. Agric. Food Chem.* **2002**, *50*, 1672–1676.

(16) Viljanen, K.; Kylli, P.; Hubbermann, E. M.; Schwarz, K.; Heinonen, M. Anthocyanin antioxidant activity and partition behavior in whey protein emulsion. *J. Agric. Food Chem.* **2005**, *53*, 2022–2027.

(17) Haslam, E. *Practical polyphenolics: from structure to molecular recognition and physiological action*; Cambridge University Press, Cambridge, 1998.

(18) Ballesteros, A.; Bornsheuer, U.; Capewell, A.; Combes, D.; Condoret, J. S.; Koening, K.; Kolisis, F. N.; Marty, A.; Menge, U.; Scheper, T.; Stamatis, H.; Xenakis, A. Enzymes in non-conventional phases. *Biocatal. Biotransform.* **1995**, *13*, 1–42.

(19) Guyot, B.; Bosquette, B.; Pina, M.; Graille, J. Esterification of phenolic acids from green coffee with an immobilized lipase from *Candida antartica* in solvent-free medium. *Biotechnol. Lett.* **1998**, *20*, 131–136.

(20) Grasso, S.; Siracusa, L.; Spatafora, C.; Renis, M.; Tringali, C. Hydroxytyrosol lipophilic analogues: Enzymatic synthesis, radical scavenging activity and DNA oxidative damage protection. *Bioorg. Chem.* **2007**, *35*, 137–152.

(21) Bouaziz, M.; Sayadi, S. Isolation and evaluation of antioxidants from leaves of a Tunisian cultivar olive tree. *Eur. J. Lipid Sci. Technol.* **2005**, *107*, 497–504.

(22) Fragopoulou, E.; Nomikos, T.; Karantonis, H. C.; Aapostolakis, C.; Pliakis, E.; Samiotaki, M.; Panayotou, G.; Antonopoulou, S. Biological Activity of Acetylated Phenolic Compounds. *J. Agric. Food Chem.* **2007**, *55*, 80–89.

(23) Myers, R. H.; Montgomery, D. C. *Response Surface Methodology: Process and Product Optimization Using Designed Experiments*; Wiley: New York, 1995.

(24) Lewis, G. A.; Mathieu, G. A.; Phan-Tan-Luu, R. *Pharmaceutical Experimental Design*; Marcel Dekker Inc.: New York, 1999.

(25) Goupy, J. *Plans d'Expériences Pour Surfaces de Réponse*; Dunod: Paris, 1999.

(26) Mosbah, H.; Sayari, A.; Mejdoub, H.; Dhouib, H.; Gargouri, Y. Biochemical and molecular characterization of *Staphylococcus xylosus* lipase. *Biochim. Biophys. Acta* **2005**, *1723*, 282–291.

(27) Ghamgui, H.; Karra-Châabouni, M.; Gargouri, Y. 1-Butyl oleate synthesis by immobilized lipase from *Rhizopus oryzae*: a comparative study between n-hexane and solvent-free system. *Enzyme Microb. Technol.* **2004**, *35*, 355–363.

(28) Gargouri, Y.; Julien, R.; Sugihara, A.; Sarda, L.; Verger, R. Inhibition of pancreatic and microbial lipases by proteins. *Biochim. Biophys. Acta* **1984**, *795*, 326–331.

(29) Mathieu, D.; Nony, J.; Phan-Than-Luu, R. *NEMROD-W* software; LPRAI: Marseille, 2000.

(30) Bouaziz, M.; Grayer, R. J.; Simmonds, M.; Damak, S. J.; Sayadi, S. Identification and antioxidant potential of flavonoids and low molecular weight phenols in olive cultivar *Chemlali* Growing in Tunisia. *J. Agric. Food Chem.* **2005**, *53*, 236–241.

(31) Capasso, R.; Evidente, A.; Avolio, S.; Solla, F. A highly convenient synthesis of hydroxytyrosol and its recovery from agricultural waste. *J. Agric. Food Chem.* **1999**, *47*, 1745–1748.

(32) Klibanov, A. M. Improving enzymes by using them in non-aqueous solvents. *J. Biol. Chem.* **2001**, *409*, 241–246.

(33) Zaks, A.; Klibanov, A. M. Enzymatic catalysis in organic media at 100°C. *Science* **1984**, *224*, 1249–1251.

(34) Krishna, S. H.; Sattur, A. P.; Karanth, N. G. Lipase-catalyzed synthesis of isoamyl isobutyrate optimization using central composite rotatable design. *Proc. Biochem.* **2001**, *37*, 9–16.

(35) Chiang, W. D.; Chang, S. W.; Shiah, C. J. Studies on the optimized lipase catalyzed biosynthesis of *cis*-3-hexen-1-yl acetate in n-hexane. *Proc. Biochem.* **2003**, *38*, 1193–1199.

(36) Foresti, M. L.; Ferreira, M. L. Solvent-free ethyl oleate synthesis mediated by lipase from *Candida antarctica* B adsorbed on polypropylene powder. *Catal. Today* **2005**, *108*, 23–30.

Received for review June 8, 2007. Revised manuscript received August 3, 2007. Accepted August 6, 2007. This work received financial support from the Ministry of Higher Education, Scientific Research and Technology in Tunisia.

JF071685Q